Journal of Applied Polymer Science

Plasticized and Nanofilled Poly(lactic acid)-Based Cast Films: Effect of Plasticizer and Organoclay on Processability and Final Properties

Marco Scatto,[1] Elena Salmini,[1] Stefania Castiello,[2] Maria-Beatrice Coltelli,[2,3] Lucia Conzatti,[4] Paola Stagnaro,[4] Leonardo Andreotti,[1] Simona Bronco[5]

[1]Centro Italiano Packaging, Via delle Industrie 25/8, 30175 Venezia Marghera, Italy
[2]Dipartimento di Chimica e Chimica Industriale, Via Risorgimento 35, 56126 Pisa, Italy
[3]SPIN-PET, Spin-off Company of the University of Pisa, Via Risorgimento 35, 56126 Pisa, Italy
[4]ISMAC-CNR UOS Genova, Via De Marini 6, I-16149 Genova, Italy
[5]Istituto per i Processi Chimico-Fisici (IPCF-CNR) Area della Ricerca, Via G. Moruzzi 1, I-56124 Pisa, Italy
Correspondence to: M.-B. Coltelli (E-mail: beacolt@ns.dcci.unipi.it) or L. Andreotti (E-mail: leonardo.andreotti@centroitalianopackaging.com)

ABSTRACT: PLA-based nanocomposites filled with the commercial organomodified montmorillonite Dellite 43B (D43B) and containing acetyl tri-*n*-butyl citrate (ATBC) as plasticizer were prepared by extrusion in a pilot-scale twin-screw extruder and melt casted into flexible films. A preliminary investigation was carried out in a laboratory batch mixer by varying blending conditions and addition procedures of the components. Indeed, the method of addition of ATBC and D43B considerably affected thermo-mechanical properties and morphology of the resultant nanocomposites. The simultaneous introduction of both ATBC and D43B during the extrusion process allowed producing clearly exfoliated nanocomposite materials with modulated mechanical and thermal properties. Moreover, rheological results, obtained during melt extrusion, assessed the processability of nanofilled-plasticized PLA, making this simple procedure interesting in view of the industrial production of nanostructured biomaterials based on plasticized PLA. © 2012 Wiley Periodicals, Inc. J. Appl. Polym. Sci. 000: 000–000, 2012

KEYWORDS: extrusion; nanocomposites; organoclay; mechanical properties; renewable resources

Received 22 March 2012; accepted 13 May 2012; published online
DOI: 10.1002/app.38042

INTRODUCTION

The development of renewable polymeric materials with modulated properties for a spread of specific applications is a subject of active research interest worldwide.[1] In this respect, aliphatic polyesters are among the most promising materials for the production of high performance environmental friendly biodegradable plastics.[2] In particular, poly(-lactic acid) (PLA) is a renewable and biodegradable polyester, which has attracted a great deal of interest in recent years. However, its thermo-mechanical and gas barrier properties cannot allow the replacement of traditional polymers in many application fields, such as films for flexible packaging. Innovative methods to modulate the properties of PLA-based materials, such as blending,[3,4] plasticization,[5] and preparation of nanocomposites,[6] need to be further developed. On the other hand, in the framework of polymer-based nanocomposites, layered silicates, such as montmorillonites (MMTs) are nanofillers largely employed in studies about the preparation of polymeric materials with modulated properties.[7]

Up to now, melt intercalation is the most investigated, and the most cost effective, method for the preparation of PLA-based nanocomposites. The effect of different organophilic modifiers onto the resultant morphology of PLA-based nanocomposites was the subject of some papers.[8–10] Di et al.[8] mixed two different organophilic MMTs (Cloisite 30B and Cloisite 93A) with a PLA matrix by using an internal mixer. Cloisite 30B is a methyl-*bis*(2-hydroxyethyl)-hydrogenated tallow quaternary ammonium modified montmorillonite and Cloisite 93A contains dimethyl-dihydrogenated tallow quaternary ammonium as modifier. The authors observed that only Cloisite 30B gave exfoliated nanocomposites. These results are in good agreement with those obtained by Krikorian and Pochan[9] for nanocomposites obtained in solution. Feijo et al.[10] compared other two commercial organo-modified MMTs (OMMTs), Dellite 43B (modified with dimethyl-benzyl-hydrogenated tallow quaternary

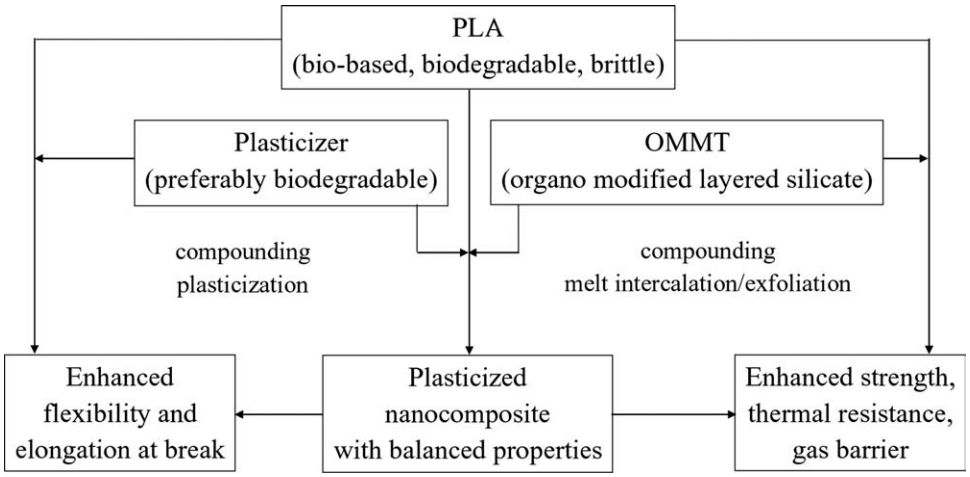

Scheme 1. Improvement of PLA properties by addition of plasticizer and/or organo modified layered silicates

ammonium) and Dellite 72T (modified with dimethyl-di(hydrogenated tallow) quaternary ammonium) for the preparation of PLA nanocomposites. The former presented a higher interaction with PLA, a slightly higher thermal stability in comparison with PLA/Dellite 72T composites. The result could be ascribed to the higher polarity of the Dellite 43B ammonium salt.

The effect of processing conditions was also considered by some authors.[11–13] Pluta[11] investigated PLA/phyllosilicates nanocomposites containing 3 wt % of Cloisite 30B prepared in a discontinuous laboratory mixer. In particular, blending time and rotor speed were varied in order to establish their effect onto morphology and properties of the resulting nanocomposites. In the experimental conditions used, they observed that (i) the molecular weight of the polymer matrix slightly decreased by increasing the blending time and (ii) the degradation of PLA was enhanced by the presence of the nanofiller. However, by increasing the rotor speed from 50 to 100 rpm only a decrease in molecular weight, without any appreciable advantage onto morphology and properties, was found. The silicate nanoplatelet dispersion was effectively enhanced by prolonging the blending time as revealed by transmission electron microscopy (TEM) analysis and dynamic frequency sweep experiments that appeared to be very sensitive to the nanostructure evolution.[11,12] Indeed, the apparent viscosity (η^*) of the unfilled PLA did not change at low frequencies, indicating a Newtonian behavior, which was then followed by a shear thinning response in the higher frequency region. The trend of η^* for the nanocomposites showed that the higher the shear thinning effect the better the resultant organoclay dispersion in the PLA matrix. Such observed trend allowed finding the concentration of organoclay able of giving a not negligible interaction between nanoplatelets. Similar results were obtained by Gu et al.[12] Moreover, Lewitus et al.[13] demonstrated the effectiveness of an approach based on a masterbatch for the preparation of PLA/Cloisite 25A (MMT intercalated with dimethyl-hydrogenated tallow-2-ethylexyl quaternary ammonium) nanocomposites with a twin screw extruder (TSE). Indeed, the preliminary preparation of a masterbatch containing a high amount (20 wt %) of OMMT and the successive melt blending with neat PLA leads to significant improvements in tensile properties of the resulting films.

A very high interest has grown recently about the plasticization of PLA[5,14,15] as well as of PLA/layered silicates nanocomposites.[16–19] This topic is particularly attractive because it can allow to improve the flexibility of PLA and properly balance mechanical and gas barrier properties of the ensuing films, as shown in Scheme 1. In particular, plasticized PLA-based nanocomposites were prepared by Paul et al.[16,17] by adding 20 wt % of poly(ethylene glycol) (PEG), having a number average molecular weight of 1000, and different amounts of unmodified or organo-modified MMT to the polymer matrix. In all cases, even for the unmodified sodium MMT (Na-MMT), intercalated nanocomposites were obtained, even though this structural organization seemed to be thermally unstable.[17] Vaia et al.,[18] confirmed this findings and claimed that PEG 1000 could intercalate preferentially in between the aluminosilicate layers of Na-MMT, leading to an increase of the interlayer distance similar to the one observed by Paul et al.[16] This selective intercalation of PEG chains was further confirmed by the impossibility of obtaining a nanocomposite by melt blending nonplasticized PLA with Na-MMT. Moreover, glassy PEG, well dispersed within the PLA matrix, exhibited also a reinforcing effect.[17]

The influence of 10 wt % acetyltriethyl citrate ester plasticizer on Cloisite 25A/PLA blown films was studied by Thellen et al.[19] WAXD and TEM investigations showed, for both compounded pellets and blown films, the intercalation of the OMMT; however, variations in screw speed and feeding rate of the TSE did not significantly affect the nanofiller dispersion and, consequently, the final properties of the resulting films. Moreover, in comparison to the neat PLA these nanocomposites showed improvements in water vapor and oxygen barrier, as well as in thermal stability and mechanical properties. Anyway, thermal behavior, such as glass transition, cold crystallization, and melting were not significantly influenced by the presence of OMMT.

By taking into account the results of this literature survey, in the present article acetyl tri-*n*-butyl citrate (ATBC) was used as

plasticizer for the preparation of PLA-based films containing 3 wt % of Dellite 43B, a commercial MMT modified with dimethyl-benzyl-hydrogenated tallow quaternary ammonium. Nanocomposites were first prepared by compounding in a discontinuous mixer following different procedures for OMMT and plasticizer addition. Then, the most promising method on the basis of morphology and mechanical properties of the ensuing composites was scaled up for the continuous extrusion by TSE. Thermal, rheological, tensile, and barrier properties, as well as the nanofiller dispersion were investigated and kept into account in order to correlate composition and processing conditions to the final properties of the resultant films. The novelty of this work consists of: (i) the optimization of the method for OMMT and plasticizer addition in a discontinuous mixer and (ii) the scale-up to a continuous one-step extrusion process by a pilot-scale TSE, which is required for the industrial application of plasticized PLA nanocomposites. To this purpose, particular attention was addressed towards outcomes and mixing factors to be taken into account for the scale-up of the process.

EXPERIMENTAL

Materials

PLA Natureworks 4042D (95.8% L-lactide, 4.2% D-lactide), MFR (190°C, 2.16 kg) 3.9 ± 0.3 g·(10 min)$^{-1}$, $\bar{M}_n$ = 183,000 g mol^{-1} was purchased from Natureworks LLC. ATBC Citroflex A4, supplied by Vertellus Chemicals, was used as plasticizer. The organo-modified montmorillonite Dellite 43B (in the following named D43B), containing about 37 wt % of dimethyl-benzyl-hydrogenated tallow quaternary ammonium, was supplied by Laviosa Chimica Mineraria.

Preparation of Nanocomposites

Preliminary laboratory scaled tests were performed in order to assess a suitable method for addition of both D43B and ATBC to PLA matrix. After drying at 60°C for 3 h under reduced pressure, PLA pellets (41 g) were melt-blended with ATBC (20 parts every 100 parts of PLA) and D43B (3 wt % of inorganic fraction on the total weight) in a counter-rotating internal mixer (Brabender OHG47055) having a mixing chamber of 50 cm^3, at the constant rotation speed of 50 rpm for 10 min. Melt blending was carried out in a dry nitrogen atmosphere to prevent thermo-oxidative degradation of PLA, the temperature, set at 180°C, increased of about 10°C during blending because of shearing. Three different procedures for the addition of OMMT and plasticizer were adopted: the first (A) consisted in the addition of D43B after 5 min of blending PLA and ATBC, the second (B) consisted in the addition of ATBC after 5 min of blending PLA and D43B, in the third (C) D43B and ATBC were added together at the beginning of the mixing. Neat PLA, PLA with D43B and PLA with ATBC were also prepared in the same conditions for comparison purposes.

Plasticized PLA films with different loading of ATBC were prepared in a pilot-scale intermeshing corotating TSE (Thermo-Haake) with the following characteristics: barrel length 960 mm, screw diameter 24 mm, and length-to-diameter ratio (L/D) 40. The screw profile (Figure 1) was composed of 10 temperature zones (each zone had L/D = 4) with three interposed kneading sections; the first kneading section started at the third temperature zone and was made up of 16 kneading discs, the second started at the seventh zone and was made up of 13 kneading discs, while the last one started at the eighth zone and was made up of 8 kneading discs. The kneading zones at different shear intensity were set up for obtaining a decreasing dispersive force along the screw profile, which should initially allow the disaggregation of nanoparticles and successively improve the dispersion of tactoids into discrete monolayers thanks to the distributive mixing action. Moreover, the decreasing shear intensity should minimize the polymer degradation. In the ninth zone there was a vent port, which was kept open during the extrusion process. A gear pump, that conveys the melt mass to a cast die, was connected to the tenth zone, between the extruder and the die. At the exit of the die the films were calandered through chill rolls set at 40°C. After several trials, the barrel temperature was set, for all the experiments, at 150°C for the first zone, at 180°C for the second zone and at 200°C for all the others, as shown in Figure 1. The die was set at 185°C.

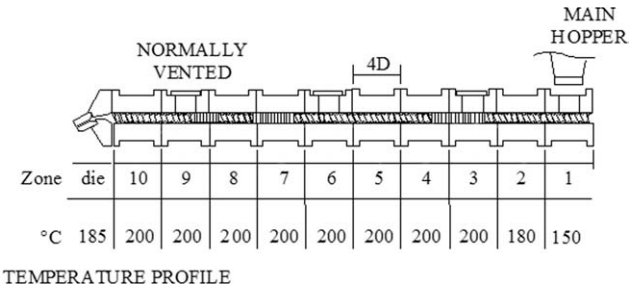

Figure 1. Screw and temperature profile used for the preparation of plasticized and nanofilled plasticized PLA in a pilot-scale intermeshing co-rotating twin screw extruder.

To evaluate how processing parameters and the amount of ATBC affected the properties of plasticized PLA film, two different screw speeds (50 and 90 rpm) were set and two compositions of plasticized PLA were prepared: PLA/ATBC 100/10 and 100/20 in weight proportion. The plasticizer was added with a peristaltic pump located in the feed zone of the extruder. The reference samples containing 10 and 20 parts of ATBC per 100 parts of PLA were labeled PLAA10R50, PLAA20R50, PLAA10R90, and PLAA20R90. Moreover, by setting the screw speed at 50 rpm, a PLA/ATBC/D43B nanocomposite of composition 80.5/16.5/3 wt/wt was prepared by feeding the organoclay to the polymer downstream with a volumetric feeder located in the feed zone of the extruder. PLA, ATBC, and D43B were mixed in the extruder in one single step. For comparison, a PLA/D43B 97/3 wt/wt nanocomposite was prepared in the same experimental conditions. Before processing PLA pellets and D43B were always dried over night at 60°C with a dry airflow (dew point −60°C, 100 dm^3 min^{-1}).

Characterizations

The melt flow rate (MFR), expressed in grams of material per 10 min, was determined with a CEAST module PIN 7026 melt flow instrument equipped with VisualMELT software, which provided melt volume rate (MVR) data. The MFR was measured at 190°C with a weight of 2.16 kg (ASTM D 1238), following the ISO1133A standard procedure. Before the MFR test, the samples were kept for 2 h at 60°C in a preheated vacuum oven to remove humidity.

Size exclusion chromatography (SEC) analyses were carried out with a JASCO chromatograph operating at a flow rate of 1 cm^3 min^{-1} and equipped with PL Gel 5 μm Mixed-D columns. The detection of molecular parameters was performed by using both a RI-2031 refractive index and an UV-2077 UV detector. Chloroform was used both as solvent and eluant.

Shear viscosities of plasticized PLA and nanofilled plasticized PLA were measured at 185°C by using an on-line capillary rheometer (OLR) placed at the end of the extruder. An exact flow of melt polymer was conveyed by a gear melt pump in a capillary at 185°C. The true shear rate $\dot{\gamma}$, true shear stress τ, and true shear viscosity η were measured varying the melt pump speed in order to change the shear rate. The range of true shear rate investigated was $\sim 100 \div 1500$ s^{-1}. Strain rates were controlled by the gear pump and chosen capillary die geometry.

The apparent shear rate ($\dot{\gamma}_{app}$) of the melt polymer into the capillary was calculated using the pump volumetric flow rate and the selected geometry of the die with the following formula [eq. (1)]:

$$\dot{\gamma}_{app} = \frac{4 \cdot Q}{\pi \cdot r^3} \quad (1)$$

where $\dot{\gamma}_{app}$ is the apparent shear rate (s^{-1}), Q is the volume stream (m^3 s^{-1}), and r is the radius of the rod capillary (m).

The apparent shear stress was calculated as it follows [eq. (2)]:

$$\tau_{app} = \frac{r \cdot \Delta p}{2l} \quad (2)$$

where l is the capillary length (m) and Δp is the pressure drop (Pa), which was measured by a pressure transducer.

The data directly obtained by the OLR are apparent values (shear rate, shear stress, and viscosity) as they inherit some faults caused by the measurement method. Therefore, the shear stress data (τ_{app}) were subjected to the Bagley correction in order to remove entrance and exit pressure drops and obtain true shear stress values (τ). The measurements were performed using two capillaries, both with a diameter of 1 mm and length of 10 and 30 mm, respectively.

To obtain true shear rate was applied the Weissenberg–Rabinowitsch correction [eq. (3)]:

$$\dot{\gamma} = \frac{\dot{\gamma}_{app}}{4} \cdot \left(3 + \frac{d \ln \dot{\gamma}_{app}}{d \ln \tau}\right) \quad \text{(for the rod capillary die)} \quad (3)$$

Finally, the true steady shear viscosity (η) (Pa s) was calculated with the following formula [eq. (4)]:

$$\eta = \frac{\tau}{\dot{\gamma}} \quad (4)$$

X-ray diffraction (XRD) patterns of Dellite 43B, PLA/D43B, and PLA/ATBC/D43B were recorded at room temperature using a Siemens Kristalloflex 810 diffractometer (Cu Kα radiation, $\lambda = 0.15406$ nm) in the 2–10° 2θ region.

The morphology of PLA/D43B and PLA/ATBC/D43B was investigated by TEM with a Zeiss EM 900 microscope applying an accelerating voltage of 80 kV. Ultrathin sections (about 50 nm thick) of compression molded samples were obtained using a Leica EM FCS cryoultramicrotome, equipped with a diamond knife, keeping the sample at −80°C.

Thermo gravimetric analyses (TGA) were performed using a Mettler Toledo TGA/SDTA 851 apparatus. TGA and derivative thermogravimetric (DTG) curves were recorded from 25 up to 600°C with a heating rate of 10°C min^{-1} under oxidative atmosphere.

Differential scanning calorimetry (DSC) characterization was carried out with a Mettler Toledo Star^e System DSC 922e Module instrument equipped with a CCA7 cooling system connected to a dewar containing liquid nitrogen. The samples (7–15 mg) recovered after blending were heated to 220°C at a rate of 20°C min^{-1} to erase any previous thermal history, then cooled to 0°C at −20°C $min^{-1}$and heated again at 10°C min^{-1} to acquire information, respectively, on crystallization and melting behavior. Measured enthalpies were normalized to the absolute weight of PLA present in the sample.

The tensile properties were tested at room temperature (27°C) with a 500 N load cell and a cross head speed of 1 mm min^{-1}. The specimens were cut from extruded cast films or compression-molded films, which were conditioned at least for 2 days at 50% relative humidity (RH) before testing.

Compression molded films (thickness about 200 μm) were prepared by using a Collin PM/20 200 press equipped with a water cooling system by heating at 200°C without pressure for 2 min, then applying a pressure of 5 MPa for 1 min and finally quenching the film at 20°C.

The oxygen permeability was measured with an Extra-Solution PermeO2 instrument at 23°C and 2.5% RH on extruded cast films (thickness about 100 μm) through an area of 50 cm^2 according to ASTM D 3985-02.

RESULTS AND DISCUSSION

Plasticized PLA

The influence of ATBC on the processability of PLA in a TSE was investigated by preparing samples (both pellets and cast extruded film) containing two different amounts of ATBC (respectively 10 and 20 parts per 100 parts of PLA). Two different screw speeds (50 and 90 rpm) were used with the temperature profile described in Figure 1. Besides the four samples labeled PLAA10R50, PLAA20R50, PLAA10R90, and PLAA20R90, neat PLA (samples PLAR50 and PLAR90) was processed in the same experimental conditions for comparison purposes.

Melt flow behavior and molecular characteristics of all the prepared samples were easily monitored by melt flow and SEC analyses, respectively (see details in Table I). The values of MFR and MVR increased by increasing the content of the liquid ATBC, while seem to be substantially independent of the screw speed. Indeed, no significant difference in the molecular characteristics of the PLA due to screw speed was found by SEC measurements (Table I).

The values of elastic modulus (E) and strain at break (ε_b) measured in tensile experiments for all the composition of plasticized

Table I. Melt Flow Properties and Molecular Characteristics of PLA and Plasticized PLA Prepared in Twin-Screw Extruder

Sample	MFR[a] g·(10 min)$^{-1}$	MVR[a] cm^3·(10 min)$^{-1}$	$\bar{M}_n^b \times 10^{-3}$ (g mol^{-1})	$\bar{M}_w^b \times 10^{-3}$ (g mol^{-1})	PDI ($\bar{M}_w/\bar{M}_n$)
PLAR50	3.8 ± 0.2	3.4 ± 0.2	96	155	1.6
PLAA10R50	8.1 ± 0.3	7.3 ± 0.3	100	157	1.6
PLAA20R50	10.7 ± 0.8	10.0 ± 0.8	100	157	1.6
PLAR90	3.6 ± 0.2	3.2 ± 0.2	111	163	1.5
PLAA10R90	7.5 ± 0.6	6.8 ± 0.6	94	155	1.6
PLAA20R90	13.4 ± 0.7	12.4 ± 0.7	99	157	1.6

[a]Determined by following ASTM D1238 and ISO1133A standard procedures.
[b]Determined by SEC (PDI = polydispersity index).

PLA, as a function of the extrusion direction, are shown in Figure 2. The tensile tests were performed on samples cut with the main axis along the direction of chill rolling (L) or perpendicular to it (T). As expected, E decreased and $\boldsymbol{\varepsilon}_b$ increased on increasing the amount of ATBC. Moreover, the sample containing 20 wt % of ATBC processed at 50 rpm showed the highest values of strain at break. As concerning the effect of extrusion direction on final properties of the films, the samples processed at 50 rpm did not show any differences; whereas, the sample PLAA20R90 showed a slightly higher strain at break in the L direction with respect to the T one. The results collected for these samples indicate that more isotropic and stable films can be prepared operating at 50 rpm.

Nanocomposites Based on Plasticized PLA

The findings obtained with the TSE for plasticized PLAs provided the basis for preliminary laboratory-scale tests for optimizing the further addition of an organo-modified MMT. Indeed, some PLA-based nanocomposites containing 20 wt % (respect to PLA) of ATBC and 3 wt % Dellite 43B (D43B), modified with dimethyl-benzyl-hydrogenated tallow quaternary ammonium, were prepared in a discontinuous internal mixer at a rotor speed of 50 rpm by adopting three different procedures: (A) addition of D43B after 5 min blending PLA with ATBC, (B) addition of ATBC after 5 min blending PLA with D43B, (C) D43B and ATBC added together to PLA at the beginning of the mixing. Neat PLA, as well as bicomponent samples of PLA with D43B and PLA with ATBC were also prepared in the same conditions for comparison purposes.

Collected torque and MFR data were reported in Figure 3 and Table II, respectively. Torque values recorded during blending showed, as expected, a neat drop of the melt viscosity in correspondence of ATBC addition, observed at about 50 s for the A and C procedure and at 300 s for the B method. MFR values confirmed that the viscosity decreased when ATBC was added to molten PLA (Table II). On the other hand a slight increase in viscosity, resulting in a reduced decrease in MFR, was observed for the binary system PLA/D43B. In the ternary systems the MFR values were comparable with those observed for plasticized PLA. Even though, when D43B was added before ATBC (method B) the MFR enhancement was higher.

On the other hand, in sample PLA/ATBC/D43B-C, where D43B was suspended in the liquid ATBC before addition, the MFR was identical to that of the corresponding plasticized PLA (PLAA20R50). Notwithstanding the complexity of the systems under investigation, the increase in the MFR values observed in samples obtained through procedures A and B could be because of the occurrence of transesterification reactions between ATBC and PLA catalyzed by the metal species present in the OMMT.[20]

Indeed, it is known that blending time is a fundamental parameter for transesterification reactions occurring in the melt.[21,22] On this basis, for the nanocomposite prepared with method C, where the permanence of both ATBC and D43B in the molten PLA

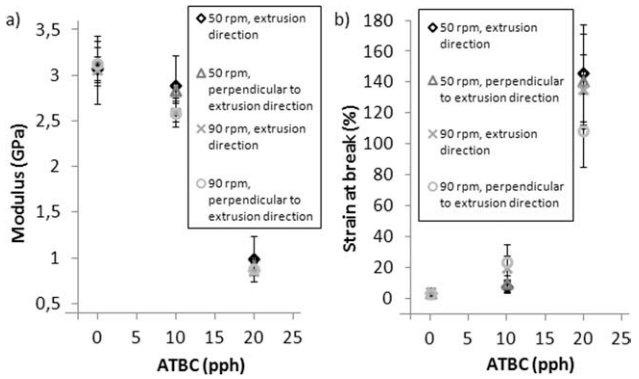

Figure 2. Behavior of elastic modulus (a) and strain at break (b) against the amount of ATBC for plasticized PLA films prepared in twin-screw extruder with different screw rates.

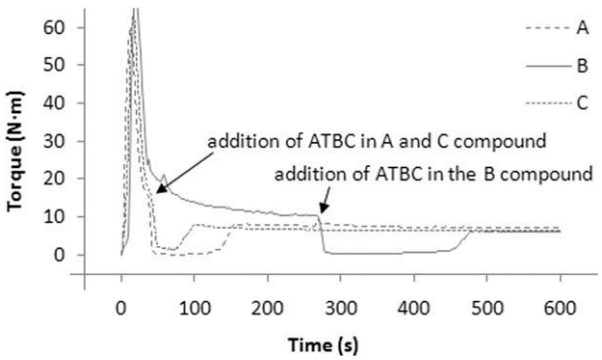

Figure 3. Torque versus time recorded during the preparation in a discontinuous mixer of PLA/ATBC/D43B nanocomposites: (A) ATBC added before D43B to molten PLA; (B) D43B added before ATBC; (C) ATBC and D43B added simultaneously.

Table II. MFR and Tensile Properties of Nanofilled Plasticized PLAs Prepared in Internal Mixer

Sample	MFR[a] (g·(10 min)$^{-1}$)	E (GPa)	σ_y (MPa)	ε_b (%)
PLA	3.9 ± 0.3	2.4 ± 0.1	63 ± 4	42 ± 9
PLA/D43B	2.4 ± 0.2	2.8 ± 0.1	59 ± 3	3 ± 0.2
PLA/ATBC	7.7 ± 0,07	2.4 ± 0.2	50 ± 5	158 ± 27
PLA/ATBC/D43B-A	9.1 ± 0.5	2.4 ± 0.2	39 ± 4	22 ± 28
PLA/ATBC/D43B-B	10.9 ± 0.4	1.3 ± 0.4	26 ± 5	199 ± 16
PLA/ATBC/D43B-C	7.7 ± 0.2	1.9 ± 0.3	37 ± 5	167 ± 55

[a]Determined by following ASTM D1238 and ISO1133A standard procedures.

during the blending was the highest, an increase of fluidity could be in principle predicted. Actually and surprisingly, this was not the case. The preliminary suspension of D43B in the plasticizer probably allowed the absorption or a strong interaction of a not negligible amount of ATBC with the nanofiller; a less amount of ATBC was thus available for plasticization and/or transesterification. This interpretation could explain the MFR results as well as the slight reduction of elongation at break and increase in elastic modulus of sample C with respect to sample B (Table II).

Tensile properties of all the prepared samples were investigated and the values of elastic modulus (E), yield stress (σ_y), and elongation at break (ε_b) were collected in Table II.

With the exception of sample PLA/ATBC/D43B-A, tensile tests showed that the addition of both ATBC and D43B was effective in determining a significant increase of the elongation at break, even with respect to plasticized PLA. In particular, the sample obtained from method B was the more ductile and that from method A was the most fragile, whereas the sample prepared through method C showed intermediate properties.

Both modulus and yield stress followed the same trend showed by elongation in the three samples; in sample C yield stress and elongation were clearly higher than the mean between corresponding values of A and B samples.

These findings cannot be attributed to a different composition of the specimens, as they were subjected to TGA tests (see below) in order to determine the actual amount of both plasticizer and filler. Thus, the observed different mechanical properties can be ascribed to the different preparation procedure.

The thermal characterization performed by TGA under air flow showed that thermal stability of the samples in terms of both onset (T_{onset}) and inflection point ($T_{i.p.}$) temperatures (Table III) was poorly improved by the addition of D43B.

Thermal behavior of all the samples was analyzed by DSC (Table III): glass transition (T_g) and melting (T_m) temperatures with related melting entalpies (ΔH_m) were determined on heating after controlled cooling from the melt, during which crystallization parameters (T_c and ΔH_c) were recorded. The glass transition of A and C samples did not change with respect to that of the reference (PLA/ATBC), whereas the B sample showed a slight T_g decrease in good agreement with tensile test data, that showed a higher ductility of B sample. Moreover, B and C samples showed T_m and T_c similar to the plasticized PLA, whereas A showed a higher T_c and lower values of related enthalpies with respect to B and C.

The dispersion of the nanoclay within the PLA matrix was analyzed by TEM and some of the pictures collected for samples PLA/D43B, PLA/ATBC/D43B-A, PLA/ATBC/D43B-B, and PLA/ATBC/D43B-C are compared in Figure 4. In all cases a very high degree of clay delamination was observed. In fact, many exfoliated layers of the clay were discernible into the PLA matrix. The presence of ATBC seemed to affect the clay dispersion as evident from observations at low magnifications. In particular, micrometric agglomerates and tactoids around the micron were observed at low magnifications in the sample PLA/ATBC/D43B-A. The presence of these aggregates could be likely responsible of the differences in the thermomechanical behavior shown by this sample with respect to those prepared with methods B and C. By adding ATBC after 5 min of blending of PLA with D43B (method B) similar micro-aggregates were present into the PLA matrix; whereas a more homogeneous distribution and a better dispersion of the clay were observed in PLA/ATBC/D43B-C.

The overall results obtained from the characterization of these samples indicated that the addition of D43B as a suspension in the plasticizer (method C) seemed to be the most promising method to scale-up in a twin-screw extruder the preparation of exfoliated nanocomposites with good final properties.

Table III. TGA Carried Out under Oxidative Atmosphere and DSC Data of Nanocomposites Based on Plasticized PLA Prepared in Internal Mixer

Sample	T_{onset} (°C)	$T_{i.p.}$ (°C)	T_g (°C)	T_m (°C)	T_c (°C)	ΔH_m[a] (J g^{-1})	ΔH_c[a] (J g^{-1})
PLA	347	366	58	152	114	24	−19
PLA/D43B	351	372	58	154	99	27	−13
PLA/ATBC	342	368	33	149	109	19	−18
PLA/ATBC/D43B-A	347	370	33	147	120	8	−9
PLA/ATBC/D43B-B	345	371	30	149	90	19	−18
PLA/ATBC/D43B-C	344	371	34	147	110	17	−19

[a]Enthalpies normalized to the absolute weight of PLA present in the sample.

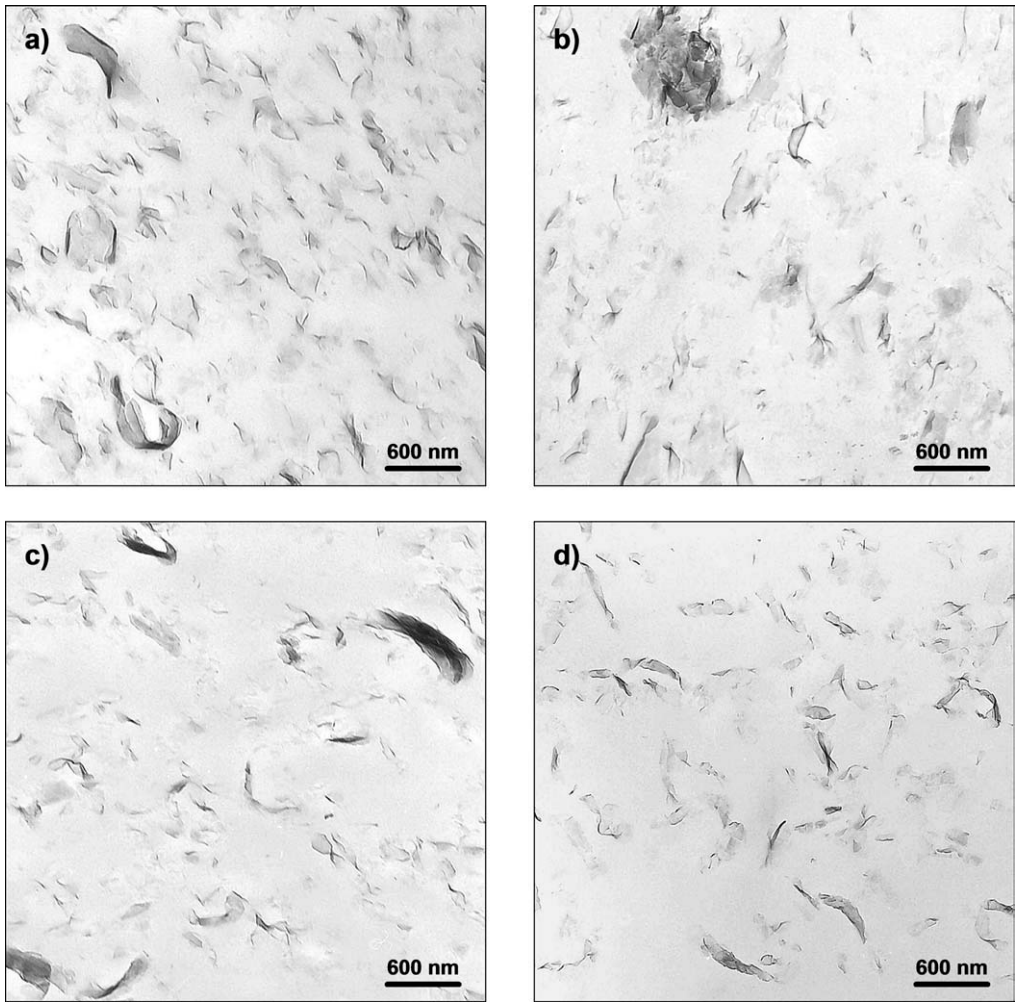

Figure 4. TEM micrographs of ultrathin sections of (a) PLA/D43B, (b) PLA/ATBC/D43B-A, (c) PLA/ATBC/D43B-B, and (d) PLA/ATBC/D43B-C, prepared in a discontinuous mixer.

On the basis of these findings, the simultaneous addition of D43B and ATBC was adopted for the preparation of a PLA-based nanocomposite containing 3 wt % of D43B and 20 wt % ATBC, with respect to PLA, by means of a pilot-scale intermeshing twin-screw extruder at a screw speed of 50 rpm. For comparison, a nanocomposite without plasticizer (PLA/D43B 97/3) was prepared in the same experimental conditions. Plasticized PLA (20 wt % ATBC) and neat PLA, previously prepared at 50 rpm (see Table I), were also taken into account.

For both PLA/D43B 97/3 and PLA/ATBC/D43B 80.5/16.5/3 samples, the resultant structural features and dispersion of the clay in the matrix were investigated by X-ray and TEM analyses.

WAXD diffraction patterns (Figure 5) showed that in both composites the intensity of the basal reflection peak of the OMMT practically disappears, suggesting a significative delamination of the organoclay.[23]

Distribution and dispersion of D43B within the PLA matrix were investigated by TEM, taking pictures, respectively, at low and high magnifications. TEM images of PLA/D43B 97/3 and PLA/ATBC/D43B 80.5/16.5/3 reported in Figure 6 indicate a good distribution of the nanoclay for both samples [Figure 6 (a, c)], even if more homogeneous in PLA/D43B 97/3 than in nanofilled plasticized PLA. A high level of organoclay's delamination was

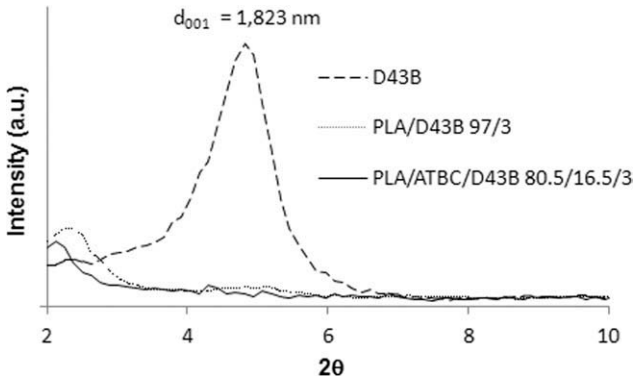

Figure 5. XRD patterns of neat D43B and nanocomposites PLA/D43B 97/3 and PLA/ATBC/D43B 80.5/16.5/3 prepared in twin-screw extruder.

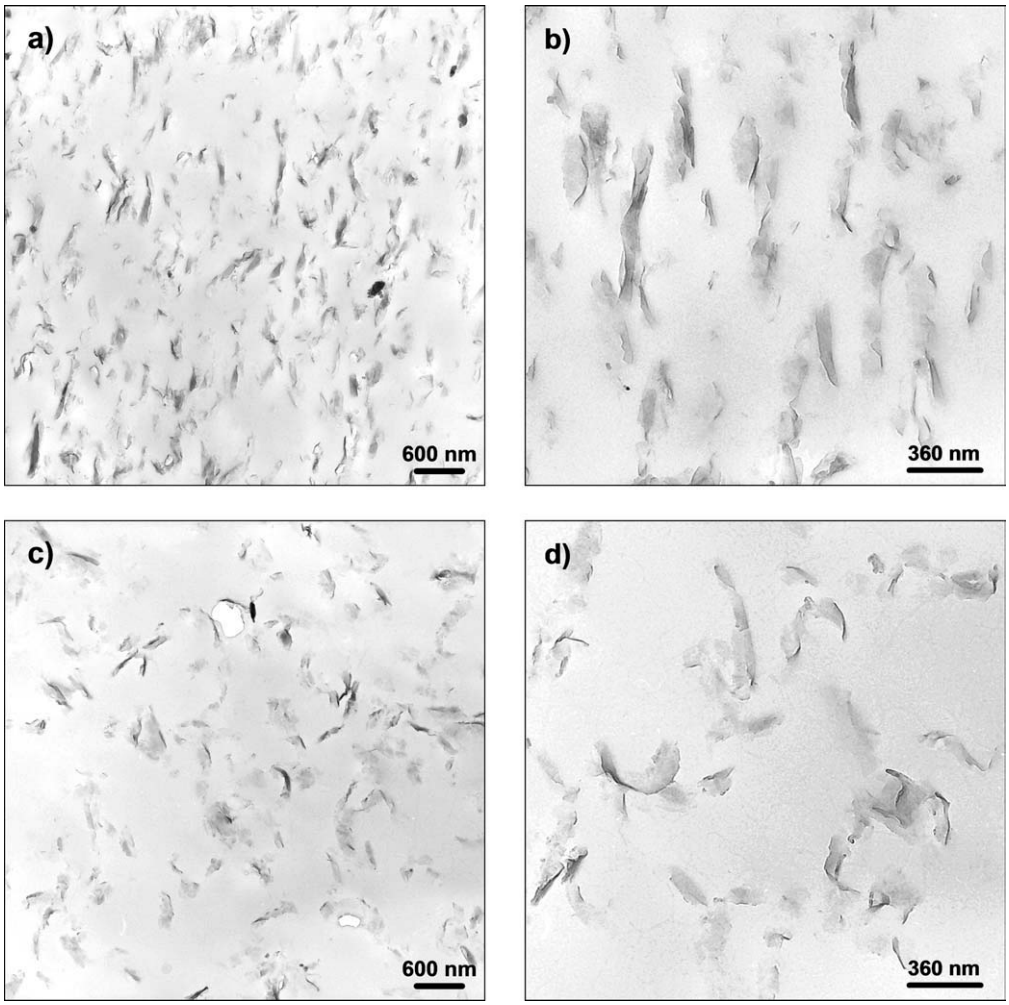

Figure 6. TEM micrographs of ultrathin sections of (a, b) PLA/D43B 97/3 and (c, b) PLA/ATBC/D43B 80.5/16.5/3 prepared in twin-screw extruder.

evidenced at higher magnification [Figure 6(b, d)]: a very large number of isolated lamellae and tactoids of few sheets were observed within the PLA matrix. TEM observations confirmed the indications obtained from WAXD analysis.

The MFR and OLR measurements carried out during the extrusion process showed, as expected, that the plasticized and the nanofilled plasticized PLA presented lower viscosity than the neat PLA (Figure 7 and Table IV); in nanofilled plasticized PLA a decrease in polymer molecular weight was revealed by SEC (Table IV). Moreover, the addition of D43B to the unplasticized PLA matrix seemed to increase the degradation of PLA polymer chains (Table IV). Indeed, the molecular weight showed a more prominent drop in nanofilled plasticized PLA with respect to nanofilled PLA. This behavior could be due to the Al alkoxydes or carboxylates present on the organoclay layers, which at high temperature could catalyze inter or intramolecular transesterification reactions. The possibility of transesterification reactions is in agreement with the observed increase in the polydispersion index (Table IV).[20–22]

The increase of MFR in the plasticized and nanofilled samples prepared in the TSE (Table IV) was higher with respect to the case of samples prepared in the discontinuous mixer (Table II). This result can be attributed to the higher impact of

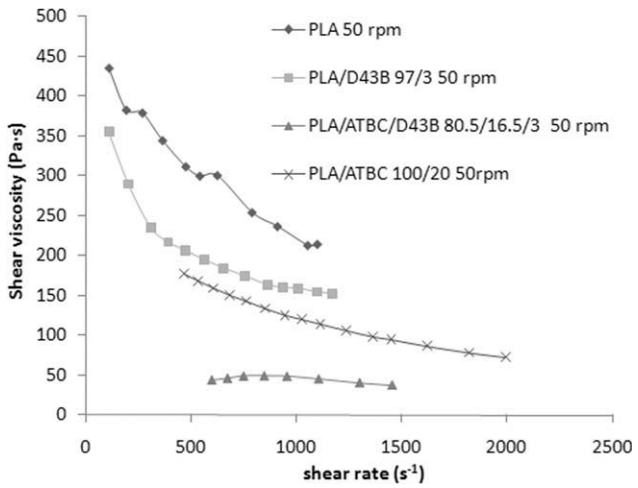

Figure 7. On-line capillary rheometer measurements of plasticized PLA and nanocomposites prepared in twin-screw extruder.

Table IV. MFR, MVR, and Molecular Characteristics of PLA and Plasticized PLA, Nanofilled PLA, and Nanofilled Plasticized PLA Prepared in Twin-Screw Extruder

Sample	MFR[a] g·(10 min)$^{-1}$	MVR[a] cm^3·(10 min)$^{-1}$	$\bar{M}_n$[b] × 10^{-3} (g mol^{-1})	$\bar{M}_w^b$ × 10^{-3} (g mol^{-1})	PDI ($\bar{M}_w/\bar{M}_n$)
PLAR50	3.9 ± 0.2	3.5 ± 0.2	101.0	161.6	1.6
PLAA20R50	10.7 ± 0.8	10.0 ± 0.8	100.0	157.0	1.6
PLA/D43B 97/3	11.4 ± 0.1	10.1 ± 0.1	59.5	121.4	2.0
PLA/ATBC/D43B	35.0 ± 0.4	32.0 ± 0.4	50.4	123.0	2.4

[a]Determined by following ASTM D1238 and ISO1133A standard procedures.
[b]Determined by SEC (PDI = polydispersity index).

transesterification in the former case, because of the higher shear stress developed during extrusion. Although the residence time in the extruder was shorter than the mixing time in the internal mixer, the screw profile set up for the extrusion allowed a higher efficiency, as shown by the improved dispersion of the nanofiller. Hence, the contact between polyester macromolecules and nanoplatelets during processing was improved by extruding, thus favoring simultaneously dispersion and reasonably decrease in molecular weight due to transesterification reactions.

The thermal stability of plasticized PLA and nanocomposites with D43B was tested by TGA under air flow. The addition of clay increased the thermoxidative stability of the PLA. For the nanocomposite with 3 wt % of organoclay, the half-decomposition temperature $T_{50\%}$, which is measured at 50 wt % mass loss, shifted up of about 11°C as compared to plasticized PLA. This behavior was probably because of an increase in the diffusion pathway length of combustion products caused by montmorillonite layers.

The DSC analysis (Table V) indicated that the presence of ATBC increased the molecular mobility of the PLA chains (lower T_g in plasticized PLA) and therefore induced the development of a higher crystallinity, as shown by the increase of the melting and crystallization enthalpy values (ΔH_m and ΔH_c, respectively) in plasticized and nanofilled plasticized PLA film. Moreover, in the unplasticized nanocomposite, the crystallization temperature was higher and the developed crystallinity was lower than those observed for the plasticized sample. Hence, the addition of both nanofiller and plasticizer allowed obtaining a material with a lower glass transition temperature with respect to neat and plasticized sample, with a higher tendency and capability of crystallizing and also a melting temperature similar to that of neat PLA.

Table V. DSC Analysis of PLA, Plasticized PLA, Nanofilled PLA, and Nanofilled Plasticized PLA Obtained in Twin-Screw Extruder

Sample	T_g (°C)	T_m (°C)	T_c (°C)	ΔH_m[a] (J g^{-1})	ΔH_c[a] (J g^{-1})
PLAR50	60	152	-	0.38	-
PLAA20R50	38	144	116	13	−12
PLA/D43B 97/3	57	152	131	2	−2
PLA/ATBC/D43B	31	151	100	21	−21

[a]Enthalpies normalized to the absolute weight of PLA present in the sample.

Organically modified montmorillonite layered silicates can act as excellent reinforcing agents for polymer materials if correctly dispersed in the polymer matrix.[7,23] Indeed, the dispersed OMMT platelets allowed the stress transfer to the high-surface area of reinforcement, strengthening, and toughening the polymeric material. This type of behavior was exhibited in our PLA/OMMT nanocomposite films. On average, the Young's modulus for the unplasticized PLA nanocomposite samples was about 10% greater than that of the neat polymer (Table VI). On the other hand, the addition of a filler to a thermoplastic matrix, even if plasticized, usually decreases significantly the elongation, but this was not the case of the nanofilled plasticized PLA film (PLA/ATBC/D43B). In fact, it showed a strain at break 14% higher than the plasticized sample, PLAA20R50 (Table VI). This result is particularly important because it keeps also into account the increase in modulus (more than 100%) showed by the reinforced and plasticized film with respect to the plasticized one.

The O_2 permeability, measured at 23°C, showed that the addition of D43B to PLA presents low barrier effect (Figure 8). Moreover, the addition of plasticizer increased significantly the permeability. The addition of D43B gave a slight decrease in permeability than the neat PLA. But the addition of both OMMT and plasticizer resulted in the increase of permeability. The result could be attributed to the decrease of molecular weight of PLA with respect to the plasticized sample. On the whole the mobility of the sample was increased because of this reaction, and this favored the diffusion of oxygen in the film.

CONCLUSION

In this study, the use of both plasticizer and nanofillers in a PLA matrix was investigated.

The preliminary study carried out onto samples prepared in a discontinuous mixer showed that the method of addition of the

Table VI. Tensile Properties of PLA, Plasticized PLA, Nanofilled PLA, and Nanofilled Plasticized PLA Obtained in Twin-Screw Extruder (Compression Molded Films from Granules)

Sample	E (GPa)	σ_y (MPa)	ε_b (%)
PLAR50	3.1 ± 0.15	49 ± 4	3.4 ± 0.9
PLAA20R50	1.0 ± 0.14	16 ± 2	143 ± 14
PLA/D43B 97/3	3.4 ± 0.2	56 ± 5	2.3 ± 0.3
PLA/ATBC/D43B	2.1 ± 0.3	34 ± 7	163 ± 35

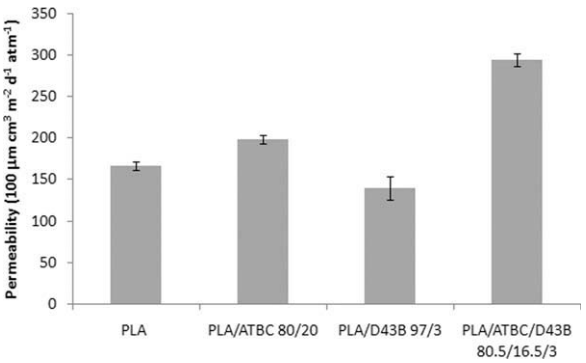

Figure 8. Permeability to oxygen of PLA, PLA/ATBC 80/20, PLA/D43B 97/3, and PLA/ATBC/D43B (80.5/16.5/3) films prepared by cast extrusion.

two additives (ATBC and OMMT) considerably affected thermo-mechanical properties and morphology of the nanocomposites. In particular, the addition of the nanofiller suspended in the plasticizer allowed obtaining an improved dispersion and a better modulation of thermo-mechanical properties.

Moreover, it was proved that the simultaneous introduction of both ATBC and OMMT during the extrusion process of nanofilled and plasticized PLA is a successful strategy to provide materials endowed with modulated mechanical and thermal properties.

Furthermore, the one step addition of ATBC and D43B is an interesting method for an industrial scale-up, in the production of plasticized PLA, even if the extrusion resulted in a more evident degradation of the polymeric matrix with respect to blending in a discontinuous mixer. Moreover, the rheological results suggested that the processability of plasticized and nanofilled-plasticized PLA is suitable for the industrial production of cast films.

The modulation of barrier properties was more difficult to be achieved and a better control onto PLA degradation should be obtained to understand the correlation of permeability tests with composition.

ACKNOWLEDGMENTS

Professor Francesco Ciardelli is thanked for helpful discussion. Financial support (NANOPACK FIRB 2003 D.D.2186 grant RBNE03R78E) by Ministero dell'Istruzione, dell'Università e della Ricerca (MIUR) is kindly acknowledged.

REFERENCES

1. Yu, L.; Dean, K.; Li, L. *Prog. Polym. Sci.* **2006,** *31*, 576.
2. Tsutsumi, N.; Kono, Y.; Oya, M.; Sakai, W.; Nagata, M. Clean Soil Air Water **2008,** *36*, 682.
3. Signori, F.; Coltelli, M. B.; Bronco, S.; Ciardelli, F. *Polym. Degrad. Stab.* **2009,** *94*, 74.
4. Coltelli, M. B.; Bronco, S.; Chinea, C. *Polym. Degrad. Stab.* **2010,** *95*, 332.
5. Coltelli, M. B.; Della Maggiore, I.; Bertoldo, M.; Bronco, S.; Signori, F.; Ciardelli, F. J. *Appl. Polym. Sci.* **2008,** *110*, 1250.
6. Sinha, R. S.; Bousmina, M. *Prog. Mater. Sci.* **2005,** *50*, 962.
7. Coltelli, M. B.; Coiai, S.; Bronco, S.; Passaglia, E. In Advanced Nanomaterials; Geckeler, K. E., Nishide, H., Eds.; Wiley-VCH: Weinheim, **2009; p 403.**
8. Di, Y.; Iannace, S.; Di Maio, E.; Nicolais, L. J. *Polym. Sci. B: Polym. Phys.* **2005,** *43*, 689.
9. Krikorian, V.; Pochan, D. J. *Chem. Mater.* **2003,** *15*, 4317.
10. Feijoo, J. L.; Cabedo, L.; Gimenez, E.; Lagaron, J. M.; Saura, J. J. *J. Mater. Sci.* **2005,** *40*, 1785.
11. Pluta, M. J. *Polym. Sci. B: Polym. Phys.* **2006,** *44*, 3392.
12. Gu, S.-Y.; Ren, J.; Dong, B. J. *Polym. Sci. B: Polym. Phys.* **2007,** *45*, 3189.
13. Lewitus, D.; McCarthy, S.; Ophir, A.; Kenig, S. J. *Polym. Environ.* **2006,** *14*, 171.
14. Piorkowska, E.; Kulinski, Z.; Galeski, A.; Masirek, R. *Polymer* **2006,** *47*, 7178.
15. Ljungberg, N.; Colombini, D.; Wesslen, B. J. *Appl. Polym. Sci.* **2005,** *96*, 992.
16. Paul, M.-A.; Alexandre, M.; Degeé, P.; Henrist, C.; Rulmont, A.; Dubois, P. *Polymer* **2003,** *44*, 443.
17. Pluta, M.; Paul, M.-A.; Alexandre, M.; Dubois, P. J. *Polym. Sci. B: Polym. Phys.* **2006,** *44*, 299.
18. Vaia, R. A.; Vasudevan, S.; Krawiec, W.; Scanlon, L. G.; Giannelis, E. P. *Adv. Mater.* **1995,** *7*, 154.
19. Thellen, C.; Orroth, C.; Froio, D.; Ziegler, D.; Lucciarini, J.; Farrell, R.; D'Souza, N. A.; Ratto, J. A. *Polymer* **2005,** *46*, 11716.
20. Albertsson, A. C.; Varma, I. K. *Biomacromolecules* **2003,** *4*, 1466.
21. Coltelli, M. B.; Toncelli, C.; Ciardelli, F.; Bronco, S. *Polym. Degrad. Stab.* **2011,** *96*, 982.
22. Conzatti, L.; Alessi, M.; Stagnaro, P.; Hodge, P. J. *Polym. Sci. A: Polym. Chem.* **2011,** *49*, 995.
23. Koh, H. C.; Park, J. S.; Jeong, M. A.; Hwang, H. Y.; Hong, Y. T.; Ha, S. Y.; Nam, S. Y. *Desalination* **2008,** *233*, 201.